Geogr. Fis. Dinam. Quat.
45 (2022). 185-195, 6 figg.

DOI 10.4461/ GFDQ.2022.45.7

LYUBA NOVI [1*], MARIA CRISTINA SALVATORE [1,2], FRANCESCO RAFFA [1],
FRANCESCA BIASCI [2], ANTONELLO PROVENZALE [1] & CARLO BARONI [1,2]

ZONATION OF WAVE-INDUCED EROSION THREAT OF A SANDY SHORELINE IN CENTRAL TUSCANY (ITALY)

ABSTRACT: NOVI L., SALVATORE M.C., RAFFA F., BIASCI F., PROVENZALE A. & BARONI C., *Zonation of wave-induced erosion threat of a sandy shoreline in central Tuscany (Italy).* (IT ISSN 0391-9838, 2022).

Coastal systems are among the most vulnerable areas on Earth, susceptible to both human and natural threats. They increasingly face detrimental effects, such as coastal erosion, exacerbated by a changing climate. Among several drivers of coastal retreat, wave action plays a crucial role, with more energetic waves potentially more disrupting. A method to assess wave-induced erosion threat distribution along coastal sectors over large scales and relevant times (i.e., > 20 yr), at high spatial resolution (i.e., < 100 m) is needed but remains elusive in the absence of high-resolution data. Wave reanalysis products with large spatio-temporal cover, do not properly resolve nearshore wave heights which are often negatively biased. The resulting underestimation of wave energy can propagate to nested models, causing an underrating of the resulting erosion. In this work, we propose a simplified method for the zonation of wave-induced erosion threat along a sandy coast, with large spatio-temporal cover and overcoming the limitations due to energy underestimation. Through a normalization procedure, long-term low-resolution data are employed in a zonation inference, without underestimating the results. The outcome is a set of two non-dimensional coefficients evaluated along the shoreline to evaluate its status. They separate over-threatened sections from under-threatened ones, when wave action is the main chronic erosion driver and human intervention is limited. The method is successfully compared with shoreline evolution measurements on a sandy coast over a 25-years period, providing a complementary assessment framework pertinent to coastal management, planning and mitigation on useful spatio-temporal scales.

KEY WORDS: Shoreline monitoring, Coastal erosion, Wave energy, Coastal risk.

RIASSUNTO: NOVI L., SALVATORE M.C., RAFFA F., BIASCI F., PROVENZALE A. & BARONI C., *Zonazione della minaccia di erosione indotta dal moto ondoso in un litorale sabbioso della Toscana centrale (Italia).* (IT ISSN 0391-9838, 2022).

I sistemi costieri sono tra le aree più vulnerabili della Terra, suscettibili alle minacce di origine antropica e naturale. Sono interessati sempre più spesso da effetti dannosi, come l'erosione costiera, esacerbati dal cambiamento climatico. Tra i diversi fattori che influenzano la regressione della linea di costa, l'azione delle onde gioca un ruolo cruciale, con onde più energiche potenzialmente più dirompenti. Un metodo per valutare la distribuzione della minaccia di erosione indotta dalle onde lungo i settori costieri su larga scala e tempi rilevanti (> 20 anni), ad alta risoluzione spaziale (< 100 m) è quindi necessario, ma rimane sfuggente in assenza di dati ad alta risoluzione. I prodotti di rianalisi delle onde con un'ampia copertura spazio-temporale non risolvono correttamente le altezze delle onde vicino alla costa, che sono spesso sottostimate. La conseguente sottostima dell'energia ondosa può propagarsi ai modelli numerici, causando una stima per difetto dell'erosione risultante. In questo lavoro, proponiamo un metodo semplificato per la zonazione della minaccia di erosione indotta dal moto ondoso lungo una costa sabbiosa, con ampia copertura spazio-temporale e superando le limitazioni dovute alla sottostima energetica. Attraverso una procedura di normalizzazione, dati a bassa risoluzione e ad ampia copertura temporale vengono impiegati in una procedura di zonazione, senza tuttavia sotto-stimarne i risultati. Ne risultano due coefficienti adimensionali valutati lungo la costa per valutarne lo stato. Essi separano le sezioni più minacciate da quelle meno minacciate, laddove l'azione delle onde è il principale fattore di erosione cronica e l'intervento antropico è limitato. Il metodo è stato confrontato con successo con misure di evoluzione del litorale di una costa sabbiosa per un periodo di 25 anni, fornendo un quadro di valutazione complementare pertinente alla gestione, pianificazione e mitigazione della costa su scale spazio-temporali utili.

TERMINI CHIAVE: Monitoraggio della linea di riva, Erosione costiera, Energia del moto ondoso, Rischio costiero.

[1] *CNR-IGG, Istituto di Geoscienze e Georisorse, Via G. Moruzzi 1, 56124, Pisa, Italy.*

[2] *Dipartimento di Scienze della Terra, University of Pisa, Via Santa Maria, 53, 56126 Pisa, Italy.*

* *Corresponding author: L. Novi (ljuba.novi.res@gmail.com)*

This study was funded by the National Research Council of Italy and the EU H2020 project ECOPOTENTIAL grant number 641762. Part of this study has been conducted using the E.U. Copernicus Marine Service Information. The work has been performed in the framework of the 32° Cycle of the PhD Course in Earth Sciences at the University of Pisa, Italy.

Authors contributions: LN conceived the study, performed the calculations, and wrote the manuscript. MCS detected the shoreline positions over 1988-2013. MCS and CB evaluated the advance and retreat of the shoreline at different time intervals. AP, FR, MCS, and CB reviewed the manuscript. FB contributed detecting some of the shoreline positions. AP provided funding.

INTRODUCTION

Coastal areas face increasing erosion and flooding due to relative sea level rise and climate change impacts. Wave action is a crucial driver of coastal erosion, as it directly influences sediment pick-up, wave-induced currents and sediments transport, with more energetic waves potentially having a greater impact (Dean & Dalrymple, 2004). Coastal erosion is likely to be enhanced by increasingly severe ocean climate conditions, with more complex effects than only coastal retreat (Irish & *alii*, 2010). Changes in wave conditions and increasing storminess can also lead to shifted sediment dynamics and increased probability of over-washing or breaching of coastal sand barriers (Wong & *alii*, 2014). These impacts are especially worrying since about 40% of the current world population lives within 100 km of the shoreline, and coastal population density is nearly three times the inland occupation (Dayton & *alii*, 2005). Owing to the inherent complexity of the nonlinear dynamics of coastal systems, however, coastal adaptation and risk management governance still remain a challenging task (Rosenzweig & *alii*, 2011). In Italy, more than 25% of sandy shorelines is currently eroding (Valpreda & Simeoni, 2003; GNRAC, 2006; Rosskopf & *alii*, 2018). Among these, the central Tuscany shoreline has received attention in recent years, mostly focused on the analysis of coastal evolution through GIS tools and photogrammetric techniques, and on specific sediment-budget issues (Anfuso & *alii*, 2011; Cammelli & *alii*, 2006; Cipriani & *alii*, 2001; Pranzini, 2001). These approaches provide useful information on evolution history and trends from a geomorphological perspective. However, they do not include a systematic analysis of long-term wave-induced threat. A necessary step for identifying appropriate risk-mitigation actions in vulnerable areas is an assessment of the shoreline sectors threatened by wave-induced chronic erosion on a relevant time span (i.e., > 20 yr) and high spatial resolution (i.e., < 100 m). Over-threatened sectors may experience stronger erosion or hindered accretion compared to under-threatened ones. Such zonation is challenging in the absence of high-resolution input parameters, detailed sedimentary characteristics and budgetary information. Due to the many factors involved, it is often necessary to collect a large amount of field wave data, historical shoreline evolution data, and geological and sedimentary data to give an accurate evaluation of past shoreline dynamics and future trends, which remain challenging at large spatio-temporal scales. The usage of numerical models for the computation of sediment transport is limited by the knowledge on the actual availability of sediments, including those of fluvial origin. However, they can still be used to quantify the physics of wave-dominated processes, but the boundary and forcing conditions need to be correctly known. High resolution wave models can be nested into coarser, large-scale and long-term models, using their output as boundary conditions. Any underestimation of the wave height boundary conditions in the coarser domain would result in underestimated modeled wave energy available for sediments displacement. This possibly leads to underestimated coastal erosion evaluations. The large spatial and temporal cover of currently available sea reanalysis is generally suitable for long-term shoreline evolution studies. However, their spatial resolution is often too coarse to resolve the details of the coastal zone, and some of the relevant parameters such as wave height may also be significantly underestimated, for example due to underestimated wind-induced wave growth (Campos & Soares, 2016). The lack of an appropriate amount of data at some locations, together with technical limitations in numerical modelling, make the zonation of wave-induced erosion threat at high spatial resolution a challenging task over broad domains. In this work, we propose a method for the zonation of a sandy shoreline to wave-induced erosion threat, which overcomes the output underestimation due to low-resolution wave heights input data. We focus on a study site in central Tuscany, Italy. The proposed approach allows to separate over-threatened coastal sectors, where the potential erosion threat (induced by average-climatological waves) is higher that the surroundings or where the accretion is weaker that the surroundings, from less-threatened ones, i.e. where the potential erosion threat is weaker than the surroundings or the accretion is stronger than the surroundings.

The zonation is verified against shoreline evolution measurements. The procedure exploits a combination of numerical simulations and spatially-coarse wave data, freely available by long-term sea reanalysis or satellite data on large spatial scales. The outcome provides two non-dimensional coefficients to separate between the long-shore wave-induced relative threat and the cross-shore wave-induced relative threat. The coefficients include the combined effects of normalized energy transport, bottom slope, wave steepness, sediment falling velocity at median diameter, and the relative orientation between breaking waves and shoreline. Such coefficients can be evaluated along a shoreline as a proxy for the associated wave-induced relative threat, without propagating the energy underestimation error to the zonation inference. We stress that the proposed methodology represents a simplification of an extremely complex system, for which a detailed quantification of each component is beyond the aims of this work. The outcome provides a useful framework for understanding past coastal changes and identifying areas to monitor, but it only accounts for wave action and, as such, it may fail when efficient human interventions or strong sedimentary input are involved.

STUDY SITE DESCRIPTION

The selected study area is a 30 km-long shoreline almost everywhere sandy, extending along the NW-SE direction of central Tuscany, Italy. Along its northern part (north of Cecina River mouth) it borders the Cecina-Rosignano coastal plain, and it extends southward to Castagneto Carducci (fig. 1). It includes mild slopes, terraced areas and coastal dunes (Aiello & *alii*, 1975; Bartolini & *alii*, 1978; Biasci, 2014). The region faces the North-West Mediterranean Sea, in a micro-tidal environment with tidal amplitudes of a few centimeters (Defant, 1961; Agresti, 2018). The chosen site is located within a single and larger coastal

physiographic unit (Lisi & *alii*, 2010) which extends from Punta Lillatro to Torre Nuova (Bowman & Pranzini, 2008). The study area does not cover the entire physiographic unit but extends between 10 km north and 20 km south of Cecina River mouth, to avoid boundaries effect that might occur at north and south open boundaries in the modeling part.

The northern area is influenced by the runoff of two rivers, Cecina River and Fine River, which represent the main sources of sediment input into this coastal system. Carbonate sediments of anthropic origin, mainly discharged by the Solvay chemical plant, additionally feed the northern beaches approximately from Punta Lillatro to Vada, which have greatly contributed to the strong coastal advancement of this sector in recent decades. Substantial urbanization has developed throughout the northern part, with tourism-related infrastructures and populated coastal towns. The area has undergone a number of changes since 1950, also due to human interventions for habitation and recreational purposes. The coastal portions from Cecina River mouth to north of Le Gorette, and along Mazzanta, have experienced a strong retreat in recent decades (qualitatively shown in fig. 2 over 1954-2013). Man-made interventions, such as shore-normal structures and a harbor, have modified these segments in recent years. South of Cecina River mouth, the shoreline covering Marina di Cecina toward Marina di Bibbona has undergone severe erosion for decades (Pranzini & *alii*, 2020). In recent years, human interventions aimed at rehabilitating Marina di Cecina urban beach have been proposed (Aminti & *alii*, 2011), acknowledging the importance of wave-induced effects on sediment transport along the beach. However, man-made interventions all along this southern part remain absent almost everywhere, i.e. from after Marina di Cecina urban beach southward to the end of the study site.

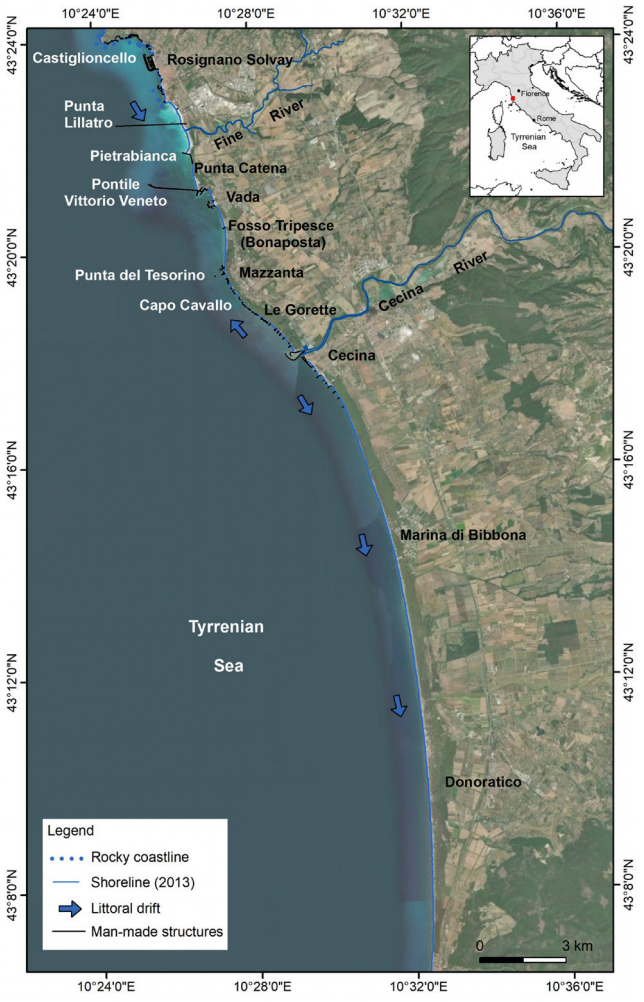

FIG. 1 - Central Tuscany study site. Detailed view (main panel) and geographic location (inside panel). The 2013-shoreline is indicated by a blue line.

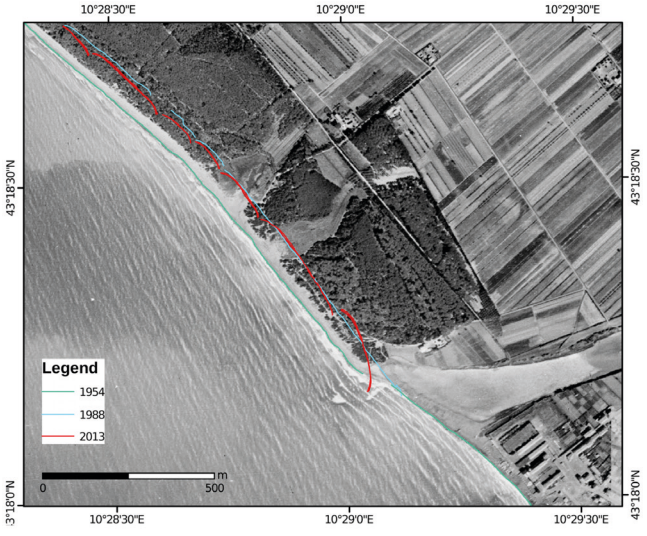

(a) 1954

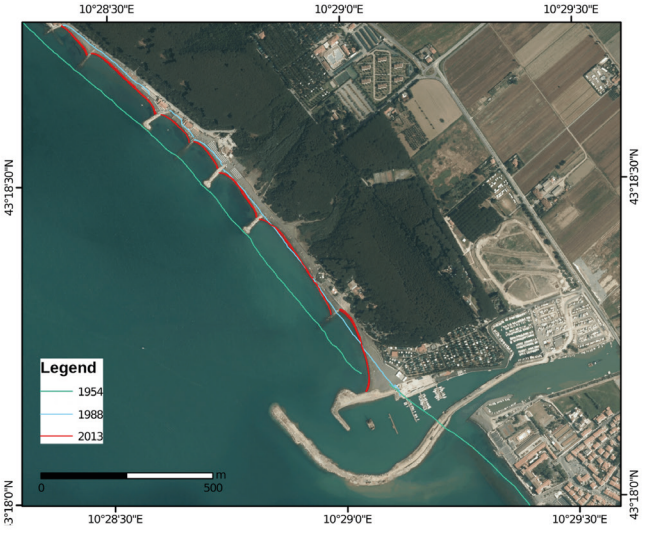

(b) 2013

FIG. 2 - Qualitative view of the coastal retreat along Le Gorette over 1954-2013. The green line in both panels shows the coastline location in 1954 (background ortophoto of panel (a)); the red line in both panels is the coastline location in 2013 (background ortophoto of panel (b)); the blue line in both panels refers to the 1988 coast.

MATERIALS AND METHODS

Zonation methodology. The procedure aims at inferring which portions of the study site face a higher wave-induced chronic erosion threat compared to the adjacent ones, from a mean climatology perspective.

The idea stems from the influence that wave action has on sediments pick-up and coastal erosion (Dean & Dalrymple, 2004), with more energetic waves potentially being stronger drivers. We build on the assumption that the dimensional wave energy transport provides a quantitative estimation of the amount of energy potentially available for the nearshore sediment uptake and displacement. We additionally consider that the quantitative reliability of the dimensional energy flux in reanalysis, which are useful to analyze large spatio-temporal scales with continuous coverage, may be affected by underestimation of the wave height in reanalysis (Campos & Soares, 2016). The proposed approach is suitable to long-term estimations of climatological averages, rather than short-term wave events such as storms, that may drive acute erosion occurrences. However, the shortness of such events allows for the application of other classical detailed approaches, such as high-resolution numerical modeling of stormy conditions, over hours or days. In such cases the amount of data and the computational resources actually needed are in fact much less and easily manageable, and therefore it will not be treated further here. The zonation methodology follows the following steps:

(i) wave seasonal climatology characterization. Wave spatio-temporal fields over the entire domain are used to characterize the area. Here, we employed the 1/8° ERAInterim reanalysis (Dee & *alii*, 2011) over 1988-2013, but other reanalysis products could be alternatively used. The analyzed parameters are significant wave height (H_s) and mean wave direction (θ_m). The wave period at spectral peak is estimated as $Tp = 5.3 \sqrt{H_s}$ following (Mangor & *alii*, 2017). To account for the spatial variability of the seasonal mean climatology we computed multi-year seasonal means of the quantities over the chosen time range in each grid point using CDO-Climate Data Operator (Schulzweida, 2022), obtaining four timesteps (one per each climatological season). Winter is defined as December, January and February, spring covers March, April and May, summer covers June, July and August, and autumn covers September, October and November. The obtained mean climatology is employed to force a set of high-resolution numerical simulations with seasonal mean climatology conditions (see point (iii)).

(ii) Identification of the closure depth d_l. It is the depth beyond which no significant seabed changes occur due to sediment transport processes; seaward of this depth the net sediment transport does not result in significant changes in mean water depth. The action of waves beyond this depth is not a major driver for the sediment motion, for orbital velocities are increasingly small toward the bottom. Along our study site, the minimum values of d_l are reported by (de Filippi & *alii*, 2008) to vary between 10.9-11.5 m and d_l = 9.1 m according to (Pranzini & *alii*, 2020), we thus assume an average value of d_l = 10.5 m here. The knowledge of d_l allows to identify the deeper meaningful limit for the evaluation of the zonation coefficients, specified along a shallow-water isobath, i.e. shallower than d_l.

(iii) High resolution seasonal mean climatology numerical modeling. The seasonal mean statistics obtained at point (i) is employed to force a set of high-resolution numerical simulations, with seasonal climatology as boundary conditions (T_p, H_s, θ_m), imposed on the model open boundaries of the coarser grid. The seasonal climatological data are spatially interpolated on the model coarser grid and, for each boundary, the maximum H_s and the corresponding T_p and θ_m (i.e., the values at the same grid point where H_s is maximum) are used as boundary condition on that boundary. The numerical model model Delft3D-WAVE (Deltares-Delft3D-WAVE, 2020) is used to transform the off-shore waves toward shallow waters, with a spatial resolution much higher than that of the input wave field. The model solves the spectral action balance equation (Hasselmann & *alii*, 1973, 1985) for the action density spectrum $E(\sigma, \theta)/\sigma$. E is the energy spectrum, σ the relative frequency as experienced by an observer moving together with the current, and θ the wave direction, i.e. perpendicular to the wave crests (Deltares-Delft3D-WAVE, 2020). The evolution equation in geometrical and spectral space accounts for the combined effects of sources and sinks for the energy density spectrum. These include energy input by wind, energy dissipation by bottom friction, whitecapping, and depth-induced wave breaking; transfer processes across scales via non-linear wave-wave interactions are also included. A detailed description of the numerical model is provided in (Deltares-Delft3D-WAVE, 2020) and references therein. The effect of bottom friction is included as a sink term for the action density spectrum equation in the empirical JONSWAP form of Hasselmann & *alii* (1973), with a bottom friction coefficient obtained by (Bouws & Komen, 1983) for fully developed wave conditions in shallow waters (0.067 m^2/s^3). The model spectral resolution is defined in frequency and directional space by a minimum and maximum frequency and a frequency resolution, and by several discrete directions. We set the minimum and maximum frequencies at 0.05 Hz and 1 Hz respectively with 24 discrete frequencies, while 36 sectors span the directional space. The spatial discretization uses a set of three nested land-boundary-fitted curvilinear grids covering the overall area, and all finer near coastal bathymetric changes. The horizontal resolution is 37×55 grid points for the external coarse grid, and 112×55 grid points for the mid-resolution grid (nested into the coarse one). To resolve the details of the coastal region, a high-resolution grid of 523×63 grid points is nested in the mid-resolution domain, to reach a maximum resolution of 29 m close to the coast (Supplementary materials fig. S6). The results will be evaluated at the highest resolution grid.

(iv) Boundary conditions on H_s, T_p, and θ_m are imposed along the model open boundaries of the overall coarser grid. We evaluated the peak period as $T_p = 5.3H^{0.5}$ according to Mangor & *alii* (2017). The model is forced

by a climatological constant wind computed according to the seasonal climatology over the considered period, i.e. averaged in time and space. Four runs are carried out to cover the four seasonal mean climatology conditions representative of the analyzed period. The resulting wave energy transport for each seasonal mean climatology is a vector Etr of amplitude *Etr*, which is then estimated on one or more different isobaths. Isobaths are chosen within the depth of closure, along the shoreline length which is measured separately on each isobath. To extract the information at the isobaths, bathymetric data are needed for the selected area. In this study we use the GEBCO gridded bathymetry dataset from The GEBCO Digital Atlas (GEBCO 2022, https://www.gebco.net/data_and_products/ gridded_bathymetry_data/). Bathymetry data are additionally interpolated on the numerical grids to serve as sea bottom morphology in the model and to compute the local bottom slope.

(v) Non-dimensional formulation and computation of the threat zonation coefficients.

To identify the coastal portions influenced by a higher wave-induced erosion threat, we derive two normalized coefficients separately for the cross-shore (*C*) and the long-shore (*L*) threats. *C* accounts for the cross-shore effects of the wave energy transport distribution along the shoreline, the bottom slope, the wave steepness, and the sediment properties. To derive *C*, we initially build on the definition of the Hattori index H_i (Hattori & Kawamata, 1980), a physically based formulation for the description of the cross-shore transport prevailing direction in the surf zone, involved in beach profile evolution related to accreting and eroding profiles. Here, we propose a local formulation for H_i and *C* starting from their formulation:

$$H_i = \frac{\left(\frac{H_0}{L_0}\right) tan\beta}{\frac{w_{s(d50)}}{gT}} \tag{1}$$

Here, H_0 and L_0 are the significant wave height and wave length outside the surf zone (just before breaking) computed by the model, $w_{s(d50)}$ is the falling velocity of median diameter grains and T is the peak period computed by the model. $tan\beta$ is the bottom slope in the surf zone, for which we give a local formulation at each grid point as $\Delta D/\Delta dc$, where *D* is the local depth positive bottom-ward, *dc* is the sea-ward distance from the shore computed along the cross-shore grid lines and Δ discrete increments refer to the numerical grid (positive increments are bottom-ward and seaward respectively). If *s* is a curvilinear coordinate defined on the i^{th} isobath, within the considered physiographic unit (within d_l but before breaking), then we define *C*(*s*) along i^{th} as

$$C(s) = \frac{\widetilde{C}(s)}{max\left(\widetilde{C}(s)\right)} \tag{2}$$

where

$$\widetilde{C}(s) = \widetilde{H}_i(s) - |min(H_i(s))| \tag{3}$$

and $\widetilde{H}_i$ is a moving-averaged smoothing of the local Hattori index evaluated along the i^{th} isobath, using local values for the bottom slope and the wave parameters. In this study we used a 5-point moving average to obtain a smoother coefficient. We will simplify the notation in the following by omitting the space dependence on *s*, keeping in mind that *C* is a space- (line-) dependent quantity. Here, *C* is interpolated on the 6.36 m isobath to carry out the zonation. We focus on non-cohesive sand with *D*50 = 0.2 mm, for which (van Rijn, 1993)

$$w_{s(d50)} = \frac{10\nu}{D50}\left(\sqrt{1+\frac{0.01\left(\varrho_{rel}-1\right)gD_{50}^3}{\nu^2}} - 1\right) \tag{4}$$

with $\rho_{rel} = \rho_{sand}/\rho_w$ the relative density of sand, ν the kinematic viscosity of water and ρ_w and ρ_{sand} the water density and sediment (sand) density respectively. In its original formulation (Hattori & Kawamata,1980) $H_i > 0.5$ ($H_i < 0.5$) corresponds to off-shore (on-shore) sediment transport, i.e. locally eroding (accreting) profiles. Here we assume that, regardless of the H_i absolute value, the higher is $\widetilde{H}_i$ the more unstable (or closer to instability) is the profile. A higher (lower) $\widetilde{H}_i$ identifies an eroding (accreting) profile or a profile more prone to erosion (accretion) if compared to sections with lower (higher) $\widetilde{H}_i$. Building on this idea, the normalized formulation of eq. 2, provides a non-dimensional proxy for the cross-shore component of the erosion threat as stated above. *C* varies between 0 and 1, where 1 corresponds to the maximum cross-shore threat, i.e. the highest $\widetilde{H}_i$, and 0 corresponds to the lowest cross-shore threat, i.e. the lowest $\widetilde{H}_i$. The higher (lower) is *C* the more (less) prone to cross-shore erosion is the local profile compared to the others. A different coefficient, *L*, is derived for the long-shore threat component. This builds on the one-line model concept (see Fredsøe & Deigaard, 1992 and references therein). It assumes that the effect of the long-shore sediment transport Q_l is an on-shore (off-shore) shifted profile resulting from erosion (accretion) and obtained by the continuity equation for sediments. If the long-shore transport is the only driver, the one-line model relates the accretion (erosion) to Q_l so that

$$\frac{\partial Y}{\partial t}(1-p)h_p = -\frac{\partial Q_l}{\partial_x} \tag{5}$$

where $\partial Y/\partial t > 0$ ($\partial Y/\partial t < 0$) identifies accretion (erosion), h_p is the active height of the profile and *p* the bed sediment porosity; $\partial Q_l/\partial x$ is the long- shore gradient of Q_l. Here, $Y > 0$ points seaward, $x = 0$ at Cecina River mouth and $x > 0$ toward Punta Lillatro. Assuming that the wave energy transport in the long-shore direction drives the long-shore sediment transport (Dean & Dalrymple,2004), the energy flux per unit length of beach, expressed as $Etr_l = Etr \cdot sin\theta_w \cdot cos\theta_w$, can be related to Q_l following Inman & Bagnold (1963) as

$$Q_l = K\frac{Etr_l}{(\varrho_{sand} - \varrho_w)g(1-p)} \quad (6)$$

typical values of p between 0.3 and 0.4, and K a dimensionless positive number. θ_w is the angle between the wave ray direction (toward which waves propagate) and the direction perpendicular to the shoreline (landward) – or between the wave crest and x – with $\theta_w > 0$ counterclockwise. Here we assume $\theta_w = \alpha_w + 90° - \delta_c$, where α_w is the angle toward which the wave ray propagates measured from East and positive counterclockwise, and δ_c is the angle the shoreline forms with the Eastward direction and positive counterclockwise.

Considering mean-climatology fields, and assuming that

$$\int_{t_1}^{t_2} \frac{\partial y}{\partial t} dt < 0$$

identifies erosion over the analyzed period $\Delta t = t_2 - t_1$, it follows from eq. 5 and 6, that erosion (accretion) over Δt occurs for $\partial Etr_l/\partial x > 0$ ($\partial Etr_l/\partial x < 0$).

Regardless of the transport intensity, a positive Etr_l gradient along x is consistent with a negative (shoreward) displacement of the mean-climatology coastal profile, i.e. climatological mean erosion induced by long-shore transport. With this assumption, we define a local long-shore non-dimensional coefficient L as

$$L = \frac{\partial_x Etr_l}{|max(\partial_x Etr_l)|} \quad (7)$$

where ∂_x denotes the gradient along x of the mean seasonal climatological Etr_l over the analyzed time range. Here we use a 8-points moving average of $\partial_x Etr_l$ to obtain a smoother curve. $L = 1$ corresponds to the maximum long-shore wave induced threat, $L > 0$ identifies over-threatened areas and $L < 0$ under-threatened ones.

The coastal zonation is then inferred through C and L as follows: the coefficients are evaluated on a shallow-water isobath shallower than d_l and deeper than the surf zone, just seaward the wave breaking. Distances are computed with the pathdist Matlab function (Green, 2022). As C and L vary along the isobath, a coastal sector is defined over-threatened if $C > C_{thr}$ or $L > 0$ or both. Otherwise, it is under-threatened. Here, C_{thr} is the 40th percentile of C.

This method is applied at the study site, comparing the resulting zonation over 1988-2013 with data of coastal evolution over the same period. Coastal changes over 1988-2013 are evaluated by a remote sensing-based approach, which uses orthophotos taken at different times over this period, available by the WMS service of the Tuscany Region portal (www.regione.toscana. it/-/geoscopio-wms, last access April 2023). The shorelines are digitized from aerial orthophotos using a Geographic Information System. Changes in shoreline position are then quantified using the Digital Shoreline Analysis System (DSAS, Himmelstoss & alii, 2018) as an ArcGIS extension. The DSAS tool computes shoreline changes at a certain point as the distance between two consecutive intersections (in the direction normal to the shoreline) of the coastal lines with a perpendicular transect. This is repeated at each defined transect, located every 50 m along the baseline.

Wave data - Hourly hindcast waves at high spatial resolution (1/24°) over the decade 2006-2016 (Korres & alii*, 2019)*

These data are used to characterize the recent wave seasonal climatology of the study site at decadal scale. The spatial resolution of 1/24° is high enough to expect the values of H_s not to be significantly underestimated offshore in terms of decadal climatology (multi-year seasonal mean). These data can therefore be used as offshore boundary conditions for the numerical model, to achieve a better representation of the shallow water effects, without expecting a strong underestimation of the computed variables. Thus, the resulting C and L coefficients can be assumed as reference values to assess the method ability to overcome the energy underestimation typical of lower (spatial) resolution data.

6-hourly ERA-Interim reanalysis at low spatial resolution (1/8°) over (a) the decade 2006-2016 and (b) the long-term period 1988-2013 (Dee & alii*, 2011)*

The reanalysis is first employed to assess that the wave energy transport underestimation (resulting by using these data) is not transmitted to the zonation coefficient inference. This is verified by comparing the zonation coefficients resulting by the usage of dataset (a) (2006-2016 at 1/8°) with the one obtained using the high-resolution data (1/24°) as boundary conditions over the same decade (see Section 4). The reanalysis is then additionally employed to carry out the coastal zonation over (b) 1988-2013, which is compared with the measured coastal evolution data over the same period.

RESULTS AND DISCUSSION

Comparison between C *and* L *estimations from low- and high-resolution input data.*

Details on the computed seasonal wave climatology and the modeled energy transport are reported in Supplementary Material. Here, we focus on the winter mean climatology (resulted more energetic) to show the underestimation obtained by the same numerical simulations when the 1/8° reanalysis are used as boundary conditions, compared to the 1/24° ones. The *Etr* winter value is computed with the same procedure in both cases, but it is everywhere dramatically underestimated if the low resolution (LR) boundary conditions apply. The maximum value along the study sectors in shallow waters is always less than about 400 W/m, against about 2000 W/m obtained with the high resolution (HR) boundary conditions.

We quantified the *Etr* underestimation as a percentage relative error $E_{r\%} = 100 \cdot (Etr_{LR} - Etr_{HR})/Etr_{HR}$ between the output obtained with the LR source dataset and with the HR one (Suppl. fig. S7). The negative values of $E_{r\%}$ are overall very intense, reaching a relative underestimation of about 97% in some areas, and never getting better than -70% throughout the field. However, the red thin bands, located close to the land boundaries, are associated to strong positive values of the percentage relative error ($E_{r\%} > 50\%$). The reason for this likely resides in

the wave-breaking processes occurring along a thin band close to the shoreline; the low-resolution data may lead to unrealistically small values of both H_s and bottom orbital velocities approaching the shoreline. This in turn may cause the wave breaking process not to be triggered or well captured in the low-resolution case. Because H_s collapses just after breaking, a local H_s overestimation may occur if the breaking process is not properly resolved. To assess that the LR underestimation does not affect the long-term zonation (carried out with LR input), we compare the coefficients computed with both LR and HR data over the time range where both the datasets overlap (2006-2016). This aims at demonstrating the applicability of the method to coarser data without losing accuracy. The scatter plots of fig. 3 compare the LR-derived L (panel a) and C (panel b) with the HR-derived ones (horizontal axis); A very good accordance is found, as measured by $R^2 = 0.99$ for C and $R^2 = 0.96$ for L. Strongly underestimated input data do not therefore affect much the C and L inference.

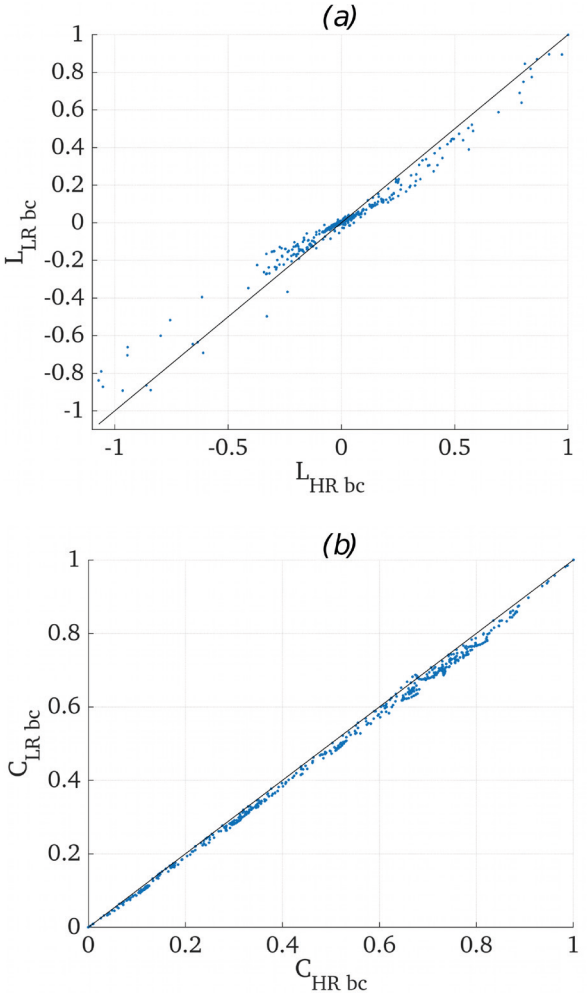

FIG. 3 - Scatter plot between (a) L computed over 2006-2016 using a high-resolution source of data for boundary conditions (L_{HRbc}) and a low resolution one (L_{LRbc}), and (b) C computed over 2006-2016 using a high-resolution source of data for boundary conditions (C_{HRbc}) and a low resolution one (C_{LRbc}). Coefficients are computed at the 6.36m isobath. The line indicates the bisector. Pearson's linear correlation coefficient is 0.98 (a) and 0.99 (b).

Inferred coastal zonation at the study site

The zonation coefficients over 1988-2013 are reported in fig. 4a for the coast south of Cecina River mouth. This region differs substantially from the coastline north of Cecina River, in terms of man-made interventions occurred over the analyzed period. Along the southern part, coastal protection structures are absent almost everywhere, while the northern part has undergone a number of interventions over the years. Therefore, the southern part is first used to assess the zonation inference under the natural threat induced by waves.

According to the zonation, two coastal sectors from 6 km to 8.2 km and from 14.2 km to 15.6 km, are classified as under-threatened, where a stronger wave-induced accretion (or weaker erosion) is expected on average. Sectors from Cecina River mouth to 6 km, from 8.2 km to 14.2 km, and from 15.6 km to 20 km are instead inferred as over-threatened, which means more prone to erosion or weaker accretion. Measured coastal displacements over 1988-2013 for the southern part are reported in fig. 4b, which display a general agreement with the inferred zonation. Areas identified as over-threatened by L and C (shadowed), experience in fact stronger erosion or weaker accretion compared to the under-threatened sectors, where the highest accretion levels are achieved instead. More quantitatively, the first over-threatened sector (from 0 km to 6 km) shows the strongest erosion pattern with a mean coastal retreat of -20.01 m (averaged over 0 km to 6 km), in agreement with the zonation inference. The central sector (8.2 km to 14.2 km), over-threatened according to the zonation, experiences the weakest mean accretion of the southern part (3.78 m averaged over 8.2 km to 14.2 km), while the southmost portion (from 15.6 km to -20 km) is on average eroding (average of -1.45 m over 15.6 km to 20 km) consistently with the over-threat zonation. Segments from 6 km to 8.2 km and 14.2 km to 15.6 km, show an average accretion of 9.53 m and 17.08 m respectively, again in agreement with the L and C inference.

The zonation inference of the northern shoreline is reported in fig. 5a and the corresponding coastal evolution measured over 1988-2013 is shown in fig. 5b (gray bars and black line for 5 points moving average). Coastline displacements over the back-ward extended period 1954-2013 are used to explore the shoreline response of those areas which has undergone protection intervention after 1988. According to the zonation, only two segments are classified as under-threatened (clear areas in fig. 5b) while four sectors as over-threatened (shadowed areas in fig. 5b). The first over-threatened sector (0 km to 2.8 km) has experienced coastal erosion over the longer period 1954-2013, where the mean shoreline retreat is -38.2 m (averaged over the sectors), in agreement with the zonation inference. The construction of protection structures and interventions in more recent years (and before 2013) have likely modified the wave-induced threat over this area, partially hampering the erosion trend (see fig. 6). The average coastal change over 1988-2013 is indeed +4.73 m. The coastal sector from 2.8 km to 5.2 km, is zonated as over-threatened according to L and C, despite somewhat weakly compared

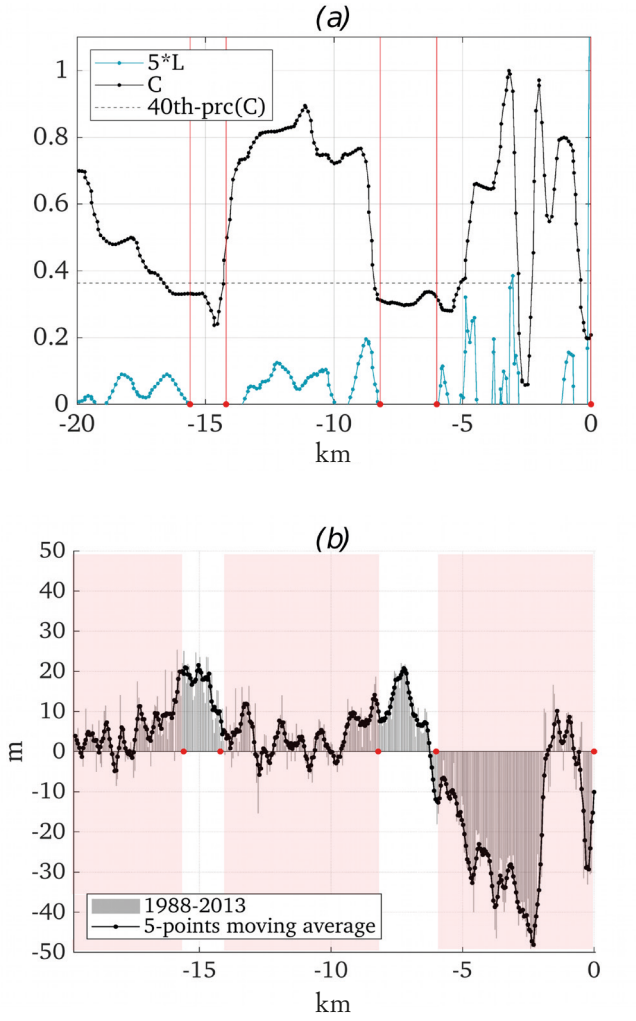

FIG. 4 - (a) Zonation coefficients over 1988–2013 south of Cecina River mouth, located at 0 km. Negative values of the horizontal axis mean southward. C is rescaled by a factor 5 to ease visualization. Red dots and vertical lines separate between over-threatened parts and under-threatened ones, as inferred by L and C. (b) Zonation inference over 1988-2013 and corresponding coastal displacements (bars). Clear areas indicate under-threatened regions. Shaded areas indicate over-threatened ones. The red dots delimit the zonation segments. Cecina River mouth is at 0 km. Negative distances along the horizontal axis mean southward.

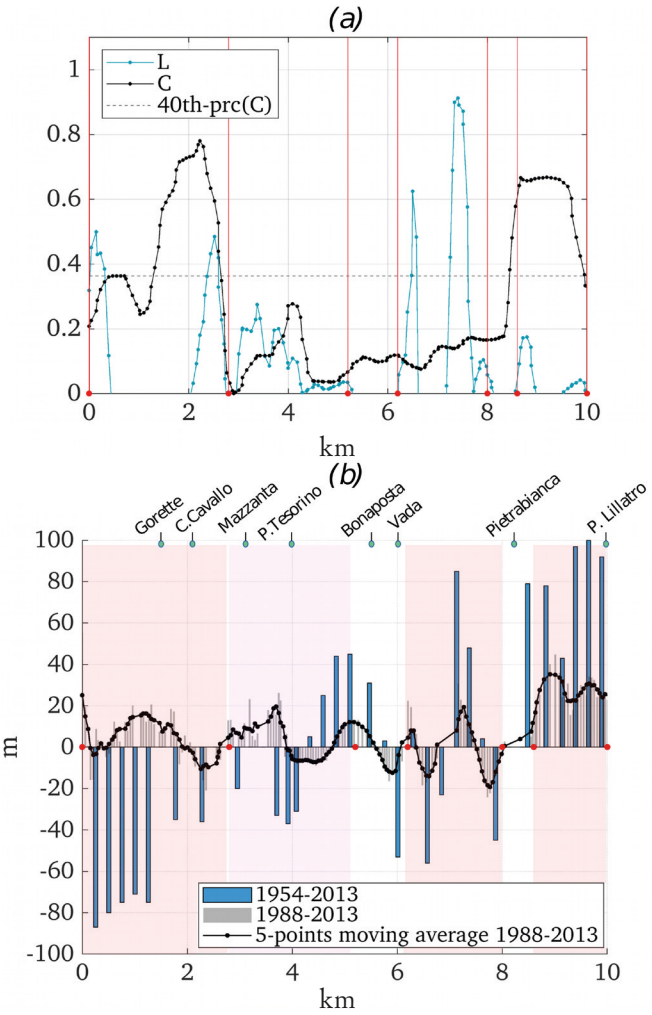

FIG. 5 - (a) Zonation coefficients over 1988-2013 north of Cecina River mouth, located at 0 km. Positive values of the horizontal axis mean northward. Red dots and vertical lines separate between over-threatened parts and under-threatened ones, as inferred by L and C. (b) Zonation inference over 1988-2013 and corresponding coastal displacements over the same period (gray bars), and over 1954-2013 (blue bars). Clear areas indicate under- threatened regions. Shaded areas indicate over-threatened ones. The red dots delimit the zonation segments. Cecina River mouth is at 0 Km. Positive distances along the horizontal axis mean northward.

to the other areas. Consistently, over 1954-2013 a weak erosion is found (-0.2 m averaged over the sector), but a weak accretion is measured over 1988-2013 instead (3.7 m averaged over the sector). Again, this shoreline portion has undergone a number of man-made changes after 1988. An example is reported in fig. 6 for the southern part of Mazzanta. Before 1988, protection structures along this part remained substantially unchanged for at least one decade (fig. 6a, b). Additional shore-parallel and shore- normal structures were built over the '90s (fig. 6c) and greatly increased until at least 2013 (fig. 6d), which may have hampered the wave induced threat resulting in a weakly accreting shoreline over 1988-2013 as opposed to 1954-2013 (eroding). Sectors from 5.2 km to 6.2 km and from 8 km to 8.6 km are zonated as under-threatened, and they consistently experienced significant accretion over 1954-2013, with averaged values of 6.6 m and 8.5 m, respectively. Accretion is also found over 1988-2013 from 8 km to 8.6 km (average 2.25 m), but a weak erosion is measured from 5.2 km to 6.2 km over this period (average 0.84 m). The shoreline portions from 6.2 km to 8 km is zonated as over-threatened, in agreement with the 1988-2013 measurements which show a mean retreat of -9.2 m averaged over the sector. Measurements over 1954-2013 show an average accretion of this sector (2.8 m) but weaker than the adjacent under-threatened sectors, in general consistently with the zonation inference. Both the 1954-2013 and the 1988-2013 coastal measurements

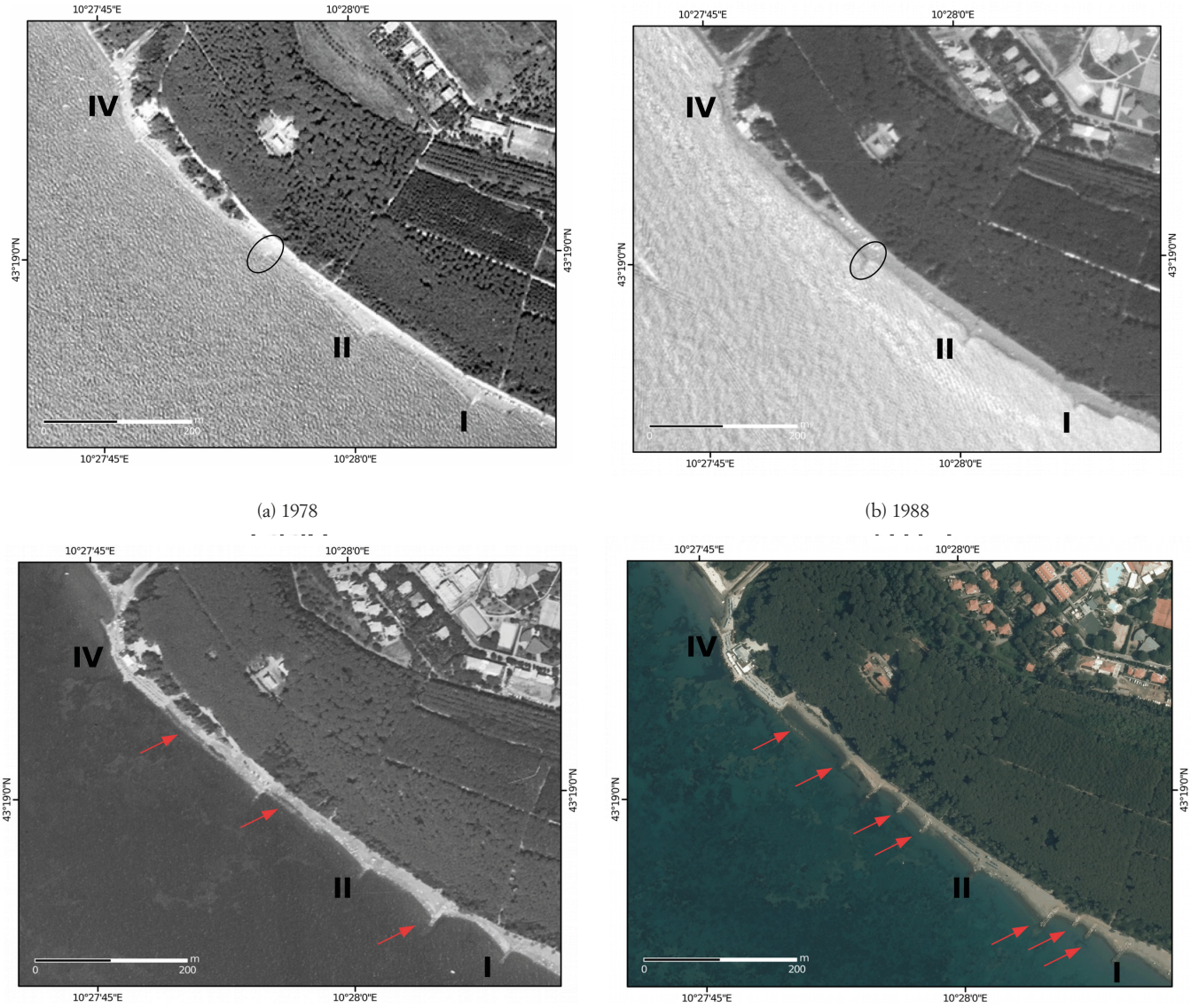

FIG. 6 - Ortophotos of segment north C.Cavallo-south Mazzanta in 1978 (a), 1988 (b), 1996 (c) and 2013 (d). The protection structures (I, II, II) arrangement remains unchanged over 1978-1988. The black circle in panels (a) and (b) shows a groyne detected in 1988 and much likely detected also in 1978. The increased protection structures after 1988 are highlighted by red arrows in panels (c) and (d).

agree on the strongly accreting behavior of the last segment (from 8.6 km to 10 km), with mean accretion values of 81.5 m and 25.9 m, respectively. The zonation inference classifies this portion as over-threatened, in disagreement with what is measured. However, this area is constantly influenced by the sediment input from Fine River and the Solvay industrial plant, which have contributed to the shoreline advancement over decades, which likely exceed the wave-induced erosion threat. As a final comment, we remark that this zonation does not account for the long-term effects of tidal advection, as it takes wave-induced processes as the major drivers for the sediment transport. In our application this assumption is justified by the very small tidal amplitudes existing in the area. These do not exceed a few centimeters at the study site, and over the whole Mediterranean Sea, where the only exceptions are the Aegean Sea, the Gulf of Gabes and the Adriatic Sea (Agresti, 2018; Defant, 1961), where resonance effects may occur. However, we have numerically verified here that the tidal- induced transport is negligible compared to the wave-induced transport, at our study location, i.e. the assumption of negligible tides when compared to the wave forcing on sediments is in line with previous knowledge on the small tidal amplitudes in the area (see Supplementary Material).

CONCLUSIONS AND PERSPECTIVES

In this work we have proposed and applied a methodology for the zonation of erosion and accretion induced by the wave mean seasonal climatology, at mid- and long-term scales, along a sandy shoreline. The method is suitable to study coastal areas where the wave action is the main forcing on sediments transport and human intervention is limited, but where high resolution wave reanalysis and detailed sedimentary data are lacking, sparse or too expensive. The resulting tool is a set of two non-dimensional coefficients which informs on the relative importance of the wave-induced threat, separating under-threatened sectors from over-threatened ones. By application at a study site in central Tuscany (Italy), the non-dimensional formulation is proved to overcome wave energy underestimations and the lack of high-resolution data. This allows to handle large periods of time at a reasonable computational cost, owing to the usage of coarse input data which doesn't reduce the accuracy of the zonation inference.

Along with the advantage of being a quick and cheap tool for large inaccessible areas based on open-source products and data, the proposed method has an inherent limitation. It is not designed to resolve the underlying physics of the complex mechanism involved in coastal morphodynamics. The long-term evolution of a shoreline is conditioned by multiple and complex processes, such as the sedimentary balance, the characteristics of the physiographic unit that underlies it, the local hydrodynamics and the anthropogenic impact, in addition to wave-induced effects. Sediment transport is a non linear function of the energy flux, thus the usage of statistical means may fails to quantify the coastal response related to individual events. The proposed approach does not presume to explain the complex interplays driving coastal dynamics by only accounting for the energy of the wave motion. Instead, it provides a simplified framework to model the average contribution of one parameter which influences the beach evolution. The comparison with objective data derived from the multi-temporal analysis of aerial images, which cover the time slot used by the model, shows that the zonation inference correctly identifies vulnerable areas along shoreline sectors where human intervention is limited. The approach presented in this work can be applied as a complementary tool to assort coastal sectors according to different levels of threat pertaining to the wave action only, to understand past changes and prioritize areas to monitor but it's not suitable for future predictions unless scenario runs are used. Future efforts will be devoted to the application of the method in other study sites, in order to gain more insight on its validity over a wider range of wave-dominated shorelines and coastal types.

SUPPLEMENTARY MATERIAL

Supplementary material associated with this article can be found in the online version, at http://gfdq.glaciologia.it/045_2_02_2022/

REFERENCES

Agresti V. (2018) - *Effects of tidal motion on the Mediterranean Sea general circulation*. Ph.D. thesis. Università di Bologna, Italia.

Aiello E., Bartolini C., Caputo C., D'Alessandro L., Fantucci F., Fierro G., Gnaccolini M., La Monica G.B., Palmieri E. L., Piccazzo M. & Pranzini E. (1975) - *Il trasporto litoraneo lungo la costa toscana fra la foce del fiume Magra ed i Monti dell'Uccellina.* Bollettino della Società Geologica Italiana, 94, 1519-1571.

Aminti P.L., Bartoletti E., Berriolo G., Bini A, Boninsegni G., Mori E., Pranzini E. & Vannucchi V. (2011) - *Marina di Cecina urban beach: a shore protection project.* Journal of Coastal Research, 10061, 282-289.

Anfuso G., Pranzini E. & Vitale G. (2011) - *An integrated approach to coastal erosion problems in northern Tuscany (Italy): Littoral morphological evolution and cell distribution.* Geomorphology, 129 (3-4), 204-214.

Bartolini C., Conedera C. & Pranzini E. (1978) - *Studi di geomorfologia costiera V: Le variazioni della linea di riva fra Rosignano e M. di Castagneto.* Bollettino della Società Geologica Italiana, 19, 353 -360.

Biasci F. (2014) - *Caratterizzazione geomorfologica ed evoluzione recente della pianura costiera tra Castiglioncello e Cecina (Livorno).* Ms.C. thesis, University of Pisa, Italy.

Bowman D. & Pranzini E. (2008) - *Shoreline monitoring: review and recommendations.* In: Pranzini E. & Wetzel L. (Eds.), Beach Erosion Monitoring, Nuova Grafica Fiorentina, 15-24.

Bouws E. & Komen G. (1983) - *On the balance between growth and dissipation in an extreme, depth-limited wind-sea in the southern North Sea*. Journal of Physical Oceanography, 13, 1653-1658.

Cammelli C., Jackson N.L., Nordstrom K.F. & Pranzini E. (2006) - *Assessment of a gravel nourishment project fronting a seawall at Marina di Pisa, Italy.* Journal of Coastal Research SI, 39, 770-775.

Campos R.M. & Soares C.G. (2016) - *Comparison and assessment of three wave hindcasts in the North Atlantic Ocean*. Journal of Operational Oceanography, 9 (1), 26-44. doi: 10.1080/1755876X.2016.1200249

Cipriani L.E., Ferri S., Iannotta P., Paolieri F. & Pranzini E. (2001) - *Morfologia e dinamica dei sedimenti del litorale della toscana settentrionale*. Studi Costieri, 4, 119-156.

Dayton P., Curran S., Kitchingman A., Wilson M., Catenazzi A., Restrepo J., Birkeland C., Blaber S., Saifullah S., Branch G., Boersma D., Nixon S., Dugan P., Davidson N. & Vörösmarty C. (2005) - *Coastal systems*. In: Hassan R., Scholes R. & Ash N. (Eds.), Ecosystems and Human Well-Being: Current State and Trends. Millennium Ecosystem Assessment Series Pt.1, Island Press, Washington DC, 513-550.

Dean R. & Dalrymple R. (2004) - Coastal Processes with Engineering Applications. Cambridge University Press, 488 pp.

Dee D.P., Uppala S.M., Simmons A.J., Berrisford P., Poli P., Kobayashi S., Andrae U., Balmaseda M.A., Balsamo G., Bauer P., Bechtold P., Beljaars A.C.M., van de Berg L., Bidlot J., Bormann N., Delsol C., Dragani R., Fuentes M., Geer A.J., Haimberger L., Healy S.B., Hersbach H., H´olm E.V., Isaksen L., Kållberg P., Köhler M., Matricardi M., McNally A.P., Monge-Sanz B.M., Morcrette J.J., Park B.K., Peubey C., de Rosnay P., Tavolato C., Thepaut J.N. & Vitart F. (2011) - *The ERA-Interim reanalysis: configuration and performance of the data assimilation system.* Quarterly Journal of the Royal Meteorological Society, 137 (656), 553-597. doi:10.1002/ qj.828

Defant A. (1961) - *Physical Oceanography.* Pergamon Press, New York, 598 pp.

Deltares-Delft3D-WAVE (2020) - *User Manual: Simulation of short-crested waves with SWAN*, available at: https://content.oss.deltares.nl/ delft3d/manuals/Delft3D-WAVE_User_Manual.pdf.

DE FILIPPI G., DUCHINI E. & PRANZINI E. (2008) - *Closure depth estimation along the tuscan coast aimed at short and long term coastal monitoring.* In: PRANZINI E. & WETZEL L. (Eds.), Beach Erosion Monitoring, Results From BEACHMED-e/Optimal Project, Nuova Grafica Fiorentina, 33-48.

FREDSØE J. & DEIGAARD R. (1992) - *Mechanics of Coastal Sediment Transport.* Advanced Series on Ocean Engineering, World Scientific, 3, 392 pp. doi: 10.1142/1546

GEBCO Compilation Group (2022) - *GEBCO_2022* Grid. doi:10.5285/e0f0bb80-ab44-2739-e053-6c86abc0289c

GNRAC (2006) - *Lo stato dei litorali italiani*. Studi Costieri, 10, 5-7.

GREENE C. (2022) - *Pathdist.* (https://www.mathworks.com/matlabcentral/fileexchange/47042-pathdist), MATLAB Central File Exchange. Retrieved November, 18 2022.

HASSELMANN K., BARNETT T.P., BOUWS E., CARLSON H., CARTWRIGHT D.E., ENKE K., EWING J., GIENAPP H., HASSELMANN D.E., KRUSEMAN P., MEERBURG A., MU¨LLER P., OLBERS D.J., RICHTER K., SELL W. & WALDEN H. (1973) - *Measurements of wind wave growth and swell decay during the joint North Sea wave project (JONSWAP).* Deutsche Hydrographische Zeitschrift, A8 (12), 95 pp.

HASSELMANN S., HASSELMANN K., ALLENDER J. & BARNETT T. (1985) - *Computations and parameterizations of the nonlinear energy transfer in a gravity wave spectrum. part ii: Parameterizations of the nonlinear transfer for application in wave models*. Journal of Physical Oceanography, 15 (11), 1378-91.

HATTORI M. & KAWAMATA R. (1980) - *Onshore-offshore transport and beach profile change*. In: EDGE B.L. (Ed.), Proceedings of 17th Conference on Coastal Engineering, Sydney, Australia, 1175-1193. doi: 10.9753/icce.v17.71

HIMMELSTOSS E., HENDERSON R., KRATZMANN M. & FARRIS A. (2018) - *Digital shoreline analysis system (DSAS) version 5.0 user guide*, U.S. Geological Survey open- file report 1179, 110 pp.

INMAN D.L. & BAGNOLD R. A. (1963) - *Littoral Processes*. In: HILL M.N. (Ed.), *The Sea*, 3, Interscience, New York, 529-533

IRISH J., FREY A., ROSATI J., OLIVERA F., DUNKIN L., KAIHATU J., FERREIRA C. & EDGE B. (2010) - *Potential implications of global warming and barrier island degradation on future hurricane inundation, property damages, and population impacted.* Ocean and Coastal Management, 53, 645-657.

KORRES G., RAVDAS M. & ZACHARIOUDAKI A. (2019) - *Mediterranean Sea waves hindcast* (cmems med-waves 2006-2017) (version 1) [data set]. Copernicus Monitoring Environment Marine Service (CMEMS). doi: 10.25423/CMCC/MEDSEA_HINDCAST_WAV_006_012

LISI I., BRUSCHI A., GIZZO M., ARCHINA M., BARBANO A., PAONE M. & CORSINI S. (2010) - *Caratteristiche della costa italiana: le unità fisiografiche e le profondità di chiusura*. L'Acqua, 2, 35-52.

MANGOR K., DRØNEN N.K., KÆRGAARD K.H. & KRISTENSEN S.E., DHI (2017) - *Shoreline Management Guidelines*. DHI Water & Environment, Hørshølm, Denmark, 449 pp.

PRANZINI E. (2001) - *Updrift river mouth migration on cuspate deltas: two examples from the coast of Tuscany (Italy)*. Geomorphology, 1-2, 125-132.

PRANZINI E., CINELLI I., CIPRIANI L. & ANFUSO G. (2020) - *An integrated coastal sediment management plan: the example of the Tuscany region (Italy).* Journal of Marine Science and Engineering, 8, 33. doi: 10.3390/jmse8010033

VAN RIJN L. (1993) - *Principles of Sediment Transport in Rivers, Estuaries and Coastal Seas. Number pt. 1.* Aqua Publications. 654 pp.

ROSENZWEIG C., SOLECKI W., BLAKE R., BOWMAN M., FARIS C., GORNITZ V., HORTON R., JACOB R., LEBLANC A., LEICHENKO R., LINKIN M., MAJOR D., O'GRADY M., PATRICK L., SUSSMAN E., YOHE G. & ZIMMERMAN R. (2011) - *Developing coastal adaptation to climate change in the New York city infrastructure-shed: process, approach, tools, and strategies*. Climatic Change, 106, 93-127.

ROSSKOPF C.M., DI PAOLA G., ATKINSON D.E., RODRIGUEZ G. & WALKER I.J. (2018) - *Recent shoreline evolution and beach erosion along the central Adriatic coast of Italy: the case of Molise region*. Journal of Coastal Conservation, 22, 879-895. doi: 10.1007/s11852-017-0550-4

SCHULZWEIDA U. (2022) - CDO user guide. URL: https://doi.org/10.5281/zenodo.7112925

VALPREDA E. & SIMEONI U. (2003) - *Assessment of coastal erosion susceptibility at the national scale: the Italian case.* Journal of Coastal Conservation, 9, 43-8.

WONG P., LOSADA I., GATTUSO J.P., HINKEL J., KHATTABI A., MCINNES K., SAITO Y. & SALLENGER A. (2014) - *Coastal systems and low-lying areas.* In: FIELD C.B., BARROS V.R., DOKKEN D.J., MACH K.J., MASTRANDREA M.D., BILIR T.E., CHATTERJEE M., EBI K.L., ESTRADA Y.O., GENOVA R.C., GIRMA B., KISSEL E.S., LEVY A.N., MACCRACKEN S., MASTRANDREA P.R. & WHITE L.L. (eds.) Climate Change 2014: Impacts, Adaptation, and Vulnerability. Part A: Global and Sectoral Aspects. Contribution of Working Group II to the Fifth Assessment Report of the Intergovernmental Panel on Climate Change Cambridge University Press, Cambridge, United Kingdom and New York, NY, USA, 361-410. doi:10.1017/CBO9781107415379.010

(Ms. received 18 November 2021, accepted 1 April 2023)